

Leeghwaterstraat 44
2628 CA Delft
P.O. Box 6012
2600 JA Delft
The Netherlands

www.tno.nl

T +31 88 866 22 00

TNO report**TNO 2016 R10262****TKI: Coatings for deliquifying gas wells**

Date	19 February 2016
Author(s)	D.H. Turkenburg J.M.C. van 't Westende
Copy no	0100294517
Number of pages	35 (incl. appendices)
Project name	TKI : Coatings for deliquifying gas wells
Project number	060.05672

All rights reserved.

No part of this publication may be reproduced and/or published by print, photoprint, microfilm or any other means without the previous written consent of TNO.

In case this report was drafted on instructions, the rights and obligations of contracting parties are subject to either the General Terms and Conditions for commissions to TNO, or the relevant agreement concluded between the contracting parties. Submitting the report for inspection to parties who have a direct interest is permitted.

© 2016 TNO

draft

Summary

Liquid loading is a well-known problem that occurs when 'wet' gas wells approach their end-of-life. Due to depletion of the reservoir, the gas flow is no longer capable in transporting all liquids to surface, hence the liquid accumulates downhole. It has been shown in previous projects that by applying a suitable coating on the tubing inner surface, this process can be delayed. The current project aimed to understand better the link between the properties of the coating and its deliquification potential.

Hypotheses have been posed, based on the results of these previous projects, to aid selecting several coatings with varying properties that have been tested from the 'microscopic' to the 'macroscopic' level. Based on this, the receding contact angle seems to be key parameter determining the performance of the coating. The coatings that are considered have a receding contact angle ranging from $\sim 55^\circ$ to $\sim 140^\circ$.

In general, the results of the tests are in line with the hypotheses:

- Increasing the hydrophobicity of a surface increases the reboundability of droplets impinging that surface. Surface roughness seems to counter this effect due to pinning.
- If the hydrophobicity of the pipe wall exceeds a critical value ($CA_{\text{rec}} > \sim 70^\circ$), the observed flow patterns change to inverted-churn flow.
- For inverted-churn flow an increase of the hydrophobicity of the pipe wall decreases the pressure gradient. The presence of an inverted-churn flow does not necessarily result in a reduced pressure gradient compared to a 'normal' churn flow.

The results of the impingement tests coincide well with those of the flow loop tests, suggesting them to be a simple and quick alternative for assessing the functionality of the coating.

From all coatings that are tested, the Fluorinated coating, having a receding contact angle of $\sim 105^\circ$, has shown the best deliquification potential: for low gas flow rates the pressure gradient is reduced significantly compared to the uncoated tubing. All other coatings did not show a significant change compared to the base case. It is noted that the onset of liquid loading itself is not significantly affected by the hydrophobicity of the pipe wall.

However, contamination of this coating with tap-water deteriorated this potential. Although this contamination seems to be removable rather easily, for applications in actual wells, where deposition is likely to be more severe, the effects of contamination puts extra limitations on coating applications.

Contents

	Summary	2
1	Introduction.....	4
1.1	Reader	4
2	History of coating studies at TNO.....	5
2.1	Game Changer I	5
2.2	Game Changer II	6
2.3	MSc thesis V.Khosla.....	6
2.4	Game Changer III	7
2.5	Game Changer IV.....	8
2.6	TKI Upstream Gas Project on Coatings for deliquifying gas wells	8
3	Working principles and coating requirements.....	10
4	Material selection and application.....	11
4.1	Classes of hydrophobic materials.....	11
4.2	Coatings based on hydrophobic materials	13
4.3	Boundary conditions for application of coatings on PMMA substrates	13
4.4	Application procedures for selected coatings.....	14
5	Coating Analysis.....	17
5.1	Contact angle measurements.....	17
5.2	Impinging droplet tests.....	18
5.3	Flow loop tests.....	19
6	Results and Discussion	21
6.1	Contact angle measurements.....	21
6.2	Droplet impingement tests	23
6.3	Flow loop tests.....	25
7	Summary and Conclusions	32
7.1	Materials	32
7.2	Coating analysis	32
8	References	34
9	Signature	35
	Appendices	
	A Droplet impingement tests	

1 Introduction

Liquid loading is a well-known problem that occurs when ‘wet’ gas wells approach their end-of-life. Due to depletion of the reservoir, its pressure drops and as a consequence the flow rates in the well drop as well. When only dry gas is present in the well the reduced flow rates have no further effect. However, when a liquid phase is present (either production fluids or condensed fluids) the reduced flow rates are not effective in transporting the liquids to topside and they will accumulate downhole (liquid loading).

In previous TNO projects (refs. 5.a to 5.d) it was found that the onset of liquid loading depends to a large extent on surface characteristics of vertical transport tubes. Material properties of the wall determine the shape and size of droplets sliding over the surface and affect the way droplets collide, bounce and stick to the surface. Changes on the microscopic level (wetting phenomena of hydrophobic and hydrophilic surfaces) escalate into effects that are well noticeable on a much larger scale. Multi-phase flow friction characteristics are changed causing eventually significant changes in the flow-regime map. It has been shown that a hydrophobic coating can reduce the pressure gradient for low gas flow rates, which can extend the production period.

In the current project a systematic study between coating properties and flow properties is performed. We aim to relate in more detail the microscopic material (mainly wetting-) properties to macroscopic flow performance of coated tubes. A multitude of materials, spanning a wide area of chemical/physical properties have been explored, ranging from strongly hydrophobic to mildly hydrophobic (but more practical in terms of application) and hydrophilic (for benchmarking). Coating properties are compared and mapped. A selection of coatings is made that is well distributed over the full range of interest. Coated sets of acrylic tubes have been subjected to lab-scale flow tests.

1.1 Reader

Chapter 2 gives a chronological overview of the various TNO projects that have led to this JIP project. The main conclusions for each project are given, showing the developments and challenges in this research. Based on the observations of these projects, in Chapter 3 a hypothesis is presented, describing how a hydrophobic coating affects the liquid loading behaviour tubes. This hypothesis is used to define which properties of the coating are relevant, and which coatings thus are candidate for assessing their potential to reduce liquid loading issues ⁽¹⁾. Chapter 4 presents the type of coating materials considered and methods to apply them on substrates. Chapter 5 and 6, describe the coating analysis techniques (including the flow tests) and their results. Concluding remarks and recommendations are given in Chapter 7.

¹ I.e. by means of decreasing the pressure gradient to the left of the minimum in the TPC and/or by shifting this minimum to lower gas flow rates.

2 History of coating studies at TNO

2.1 Game Changer I

The study to the effect of coatings on the onset of liquid loading at TNO started in 2009 with the Shell Liquid Loading Game Changer I project (ref. 5.a). This literature research concluded that the onset of liquid loading was caused by flow reversal in the liquid film and not by entrained droplets (Westende, ref. 8). Two concepts to postpone the onset of liquid loading to smaller gas flowrates have been analyzed : (1) transforming all liquid into droplets, or (2) manipulating the liquid film.

The first concept is judged not feasible due to the high pressure drops in the system (due to the high shear that is required to create droplets small enough to avoid deposition). The second concept results manipulation of the wall by means of : (a) applying coatings on the pipe wall (Takamasa 2008), or (b) applying local obstructions on the wall (no literature found).

Takamasa (ref. 6) performed experiments in a vertical test loop with various coatings ⁽²⁾. They found a change in flow pattern when a hydrophobic coating was applied : inverted-churn flow at low gas flowrates and droplet flow at 'high' gas flowrates (see Figure 2.1). With the hydrophobic coating, the liquid is completely detached from the pipe wall for both flow patterns. With a hydrophilic coating the observed flow patterns are equal to those observed in the base system (acrylic pipe), but the churn-annular transition shifted to lower gas velocities. They did not report significant changes to the pressure gradient. TNO found in experiments that the pressure drop could decrease when applying a hydrophobic coating on the pipe wall.

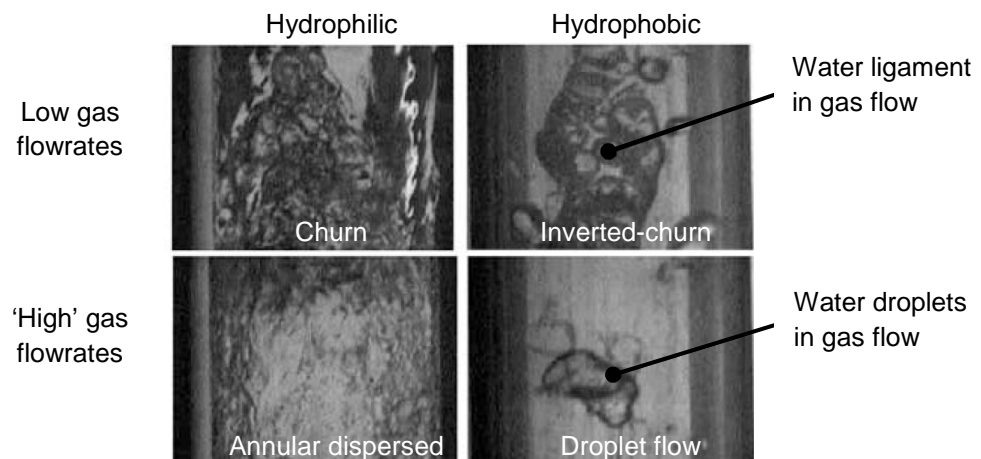


Figure 2.1 Flow visualisation of air/water flow in an acrylic pipe with hydrophilic (left) and hydrophobic (right) coating applied on the pipe wall. The top images are for low flow rates ($U_{sg} = 3.3$ m/s, $U_{sl} = 0.3$ m/s), and the bottom images are for 'high' flow rates ($U_{sg} = 10$ m/s, $U_{sl} = 0.1$ m/s). Taken from Takamasa (ref. 6).

² Air/water, ID = 20mm, L = 2.8m. $CA_{hydrophobic} \approx 135^\circ$, $CA_{acrylic} \approx 45^\circ$, $CA_{hydrophilic} < 7^\circ$. They measured with relative low gas flow rates ($F_g = U_{sg}/\sqrt{(gD)} \sqrt{(\rho_g/\Delta\rho)} < 0.8$, and high loading (LGR $> 50,000 \cdot 10^{-6} \text{ m}^3/\text{Sm}^3$)

2.2 Game Changer II

In the Shell Liquid Loading Game Changer II (refs. 5.b and 7) the effect on liquid loading by manipulating the liquid film has been assessed through experiments. This manipulation has been achieved by: (a) applying a coating on the pipe wall, (b) applying taper, or (c) using an orifice (see Figure 2.2).

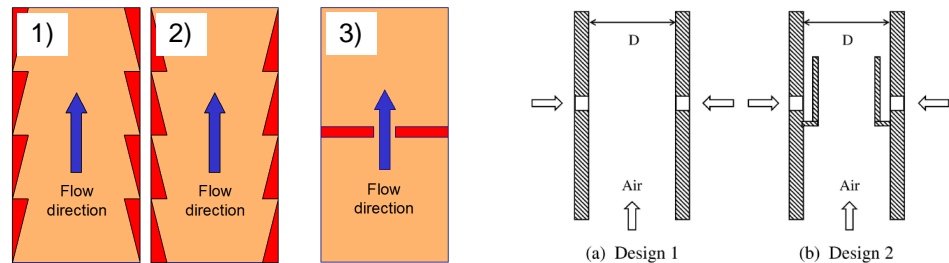


Figure 2.2 Left : Schematic of pipe wall manipulation alternatives : 1) taper up, 2) taper down, and 3) orifice. Right: Schematic of liquid injection designs of V.Khosla (ref. 3).

The experimental setup is a vertical pipe with an ID of 20mm and a length of 3m. Dry air is injected at the bottom and ultra pure water is injected 1050mm above the gas inlet via 2 small ID holes. Gas and water flows are both mass flow controlled. The outlet of the pipe is kept at atmospheric conditions. The coating tests have been performed using : 1) cleaned RVS (hydrophilic, $CA = \sim 0^\circ$), 2) untreated RVS (base case, $CA = \sim 60^\circ$) and 3) a Fluor-based coating⁽³⁾ on RVS tubing (hydrophobic, $CA = \sim 140^\circ$). The taper and orifice experiments used acrylic tubing. The gas flow rates varied from $2 < U_{sg} < 40$ m/s and the liquid flow rates varied between $0 < U_{sl} < 8.84$ cm/s (i.e. resulting in $0 < LGR < 10,000 \cdot 10^{-6} \text{ m}^3/\text{Sm}^3$).

The conclusions are that applying a hydrophobic coating on the pipe wall seems the most promising technique for deliquification: the minimum stable gas flow rate is reduced as well as the pressure drop at this flow rate. Note, however, at high gas flow rates the pressure drops are increased when a hydrophobic coating is applied. Also, it is noted that the onset of liquid loading is not affected.

2.3 MSc thesis V.Khosla

TNO and TUDelft jointly performed a visual investigation of the effects of applying a Fluor-based coating on liquid loading (refs. 3 and 4). This experimental study was performed using two flow loops : a small scale flow loop and a large scale flow loop. They use the minimum in the TPC to predict the lowest stable gas flow.

Small scale flow loop

The small scale flow loop is an acrylic pipe with an ID of 20mm and a length of 3m. Dry air is injected at the bottom and ultra pure water is injected 22D above the gas inlet. Two liquid inlet section have been tested : 1) design I where the water is introduced via 4 small ID holes and 2) design II where water is injected via an arrangement of concentric pipes to allow faster development of the liquid film at the

³ TNO has developed a heavily-fluorinated in-house synthesized polymer, which has a high amount of CF_3 end groups.

wall, see Figure 2.2 ⁽⁴⁾. The outlet of the pipe is kept at atmospheric conditions. Pressures are measured at 90D and 135D from the pipe inlet.

Large scale flow loop

The large scale flow loop is an acrylic pipe with an ID of 50mm and a length of 13m. Dry air is injected at the bottom and tap water is injected ~20D above the gas inlet (design II). The outlet of the pipe is kept at atmospheric conditions. Pressures are measured at 180D and 220D from the pipe inlet. The liquid holdup is measured using fast shut-off valves located at 80D and 240D from the pipe inlet.

The main conclusions with respect to the effects on liquid loading by applying a hydrophobic coating are:

- The flow patterns change, similarly as has been observed by Takamasa (ref. 6).
- The minimum in the TPC curve shifts to lower U_{sg} . In the large scale flow loop, this effect decreases with increasing U_{sl} to zero
- At high U_{sg} , the pressure drop becomes larger, this effect increases with U_{sl} to a maximum of ~20%.
- The liquid holdup decreases (i.e. the liquid travels faster).
- The onset of liquid loading is affected only slightly (the exact design of the liquid feed has a more pronounced effect : design II results in a smaller U_{crit}).

2.4 Game Changer III

In the Shell Liquid Loading Game Changer III (ref. 5.c) the effect on liquid loading by changing the pipe wall wettability has been investigated further. Experiments have been performed with a Fluor-based coating at an industrial scale flow loop (Shell Donau loop). Additionally, the 3 pipe wall treatments of Game Changer II are compared against 3 alternative 'wall-treatments' in a laboratory setup.

Industrial scale tests

The Mast test section of the Shell's multiphase flow facility in Rijswijk (generally referred to as the Donau loop) is used to mount the flow loop onto. The piping of the flow loop has an ID of 67mm and a total length of 12m. The piping was made of RVS, with and without a Fluor-based coating. Air and water (either single pass process water or circulating drinking water) are mixed just upstream of the inlet of the flow loop. The air flow varied from 0 to ~58m/s (at atmospheric conditions) and the LGR varied from ~100 to $4500 \cdot 10^{-6} \text{ m}^3/\text{Sm}^3$. The pressure was varied from atmospheric to 3 barg. Experiments have been performed with a vertical and 45° inclined orientation.

The overall conclusion of the industrial scale tests is that a difference in liquid loading behavior was not observed between cleaned RVS and coated RVS. The reason for this is that the wettability of the pipe wall by the coating has changed during the testing : $CA_{stat} : 124^\circ \rightarrow 105^\circ$, $CA_{adv} : 121^\circ \rightarrow 100^\circ$, $CA_{rec} : 104^\circ \rightarrow 0^\circ$.

Probable causes for this change in the industrial scale tests are given as :

- Partially damaged/removed coating.
- Appearance of pinholes (leaving the static and advancing CA intact, but decreasing the receding CA significantly).

⁴ Design I has an onset of liquid loading at higher gas flow rates than design II, since the arrangement of concentric pipes in design II results in an effective smaller pipe diameter.

- Difference in type of water used in the industrial setup compared with that used in the laboratory setups in previous projects. However, this is shown not to be the main cause ⁽⁵⁾.

Laboratory scale tests

In a laboratory setup (see Game Changer II, section 2.2) the 3 pipe wall treatments of Game Changer II (cleaned RVS, untreated RVS and Fluor-based coating on RVS) are compared against 3 alternative 'wall-treatments' :

- Twister (μ -structure) ($CA_{stat} = \sim 96^\circ$, $CA_{adv} = \sim 99^\circ$, $CA_{rec} = \sim 85^\circ$),
- Shell Houston coating ($CA_{stat} = \sim 113^\circ$, $CA_{adv} = \sim 123^\circ$, $CA_{rec} = \sim 83^\circ$)
- Corrosion inhibitor ($CA_{stat} = \sim 51^\circ$, $CA_{adv} = \sim 51^\circ$).

The overall conclusion of the laboratory scale setup with various coatings is that an postponing of the onset of liquid loading is only observed for the Fluor-based coating developed by TNO. It seems that a minimum receding contact angle of 100° is required to show any effect on the liquid loading behavior.

2.5 Game Changer IV

In the Shell Liquid Loading Game Changer IV (ref. 5.d) the effect of pipe inclination on the performance of a hydrophobic coating is studied. Experiments have been performed with an uncoated and coated acrylic pipe with an ID of 20mm and length of 3m. Dry air is injected at the bottom and ultra pure water is injected ~ 300 mm above the gas inlet via 2 small ID holes. Gas and water flows are both mass flow controlled. The outlet of the pipe is kept at atmospheric conditions. The pipe inclination is varied from vertical to near horizontal (10°). The gas flow rates varied from $4 < U_{sg} < 40$ m/s and LGR-values used are : LGR = 200, 1000 and $4000 \cdot 10^{-6} \text{ m}^3/\text{Sm}^3$.

The overall conclusion of the laboratory scale setup are :

- Applying a hydrophobic coating changes the flow patterns.
- Applying a hydrophobic coating shifts the minimum in the TPC to lower gas flow rates.
- The effect of coating diminishes with increasing LGR.
- The effect of coating diminishes with decreasing inclination (from horizontal).
- Coating adherence problems have not observed in the project.

Proof of concept is considered given in Game Changer projects I through IV (summarized in ref. 1). It is recommended to continue with the proof of application, focusing on field conditions (HCs, sand, real production tubing).

2.6 TKI Upstream Gas Project on Coatings for deliquifying gas wells

As described above, TNO has performed a number of studies on liquid loading of gas wells and the mitigation of liquid loading. In one of these studies, commissioned by NAM, the use of a hydrophobic coating for mitigation of liquid loading was

⁵ A cross-check with the laboratory scale setup on the effect of water using purified water and tap water has been performed, indicating that purified water moves more easily along the coated surface. This is however a too small effect to explain the observed differences.

proposed. In subsequent studies (funded through the Shell game-changer program) the principle was further demonstrated.

From these projects, Shell Patent Application WO2011073204 (A1), filed on 2011-06-23 by Kees Veecken, has emerged. This patent describes the use of hydrophobic coatings for gas well deliquification. A licence to this patent is essential for development and implementation of this innovative idea.

In the current project, the idea is further investigated in order to identify a coating that shows the desired mitigation effect while enduring down-hole gas well conditions for an extended period of time.

The in-kind contribution of Shell consists of a fully paid-up, perpetual, irrevocable, non-exclusive, non-transferable licence to the Shell Patent WO2011073204 without the right to grant sublicenses, which license is granted to all other JIP participants. The in-kind contribution of Shell amounts to a total contribution fee of EURO 18.750,00 (eighteen-thousand-seven-hundred-fifty).

Without this contribution, the right to use the patent within its application field, the project could not have been performed.

3 Working principles and coating requirements

In the previous projects it is observed that by applying a hydrophobic coating on the pipe wall the liquid gets detached from the wall. This results in a redistribution of the liquid in the flow (i.e. a change in flow pattern). For moderate/low gas flow rates the flow pattern changes from churn-annular to inverted-churn flow and for high gas flow rates the flow pattern changes from annular to droplet flow.

In order to prevent a liquid film to reform, droplets impacting on the pipe wall may not remain and accumulate there, but they should be re-entrained into the gas core. When the droplets impact and rebound with the pipe wall more elastically, this re-entrainment is improved. Also, a more elastic interaction of the droplets with the wall results in a reduction of the momentum-loss to the wall ⁽⁶⁾. This in turn causes the pressure gradient to be lower and the liquid phase velocity to be higher, which again lowers the liquid holdup.

The rebound of a droplet from a surface is considered to be more elastic (i.e. a better 'reboundability'), when the droplet sticks less well to this surface. This 'stickiness' of a surface has been related to the receding contact angle (i.e. the contact angle at the tail of a droplet sliding down an inclined surface) ⁽⁷⁾.

Hypotheses

- I. Increasing the receding contact angle, increases the reboundability of droplets impinging on a surface.
- II. Increasing the reboundability of droplets from the pipe wall reduces the accumulation at the wall (i.e. reduces film formation), causing a change in flow patterns
- III. Under conditions of droplet flow or inverted-churn flow, a more elastic rebound of droplets, reduces the momentum-loss to the wall, hence reduces the pressure gradient ⁽⁸⁾.

Based on the above hypotheses, it is attempted to make coatings over a range of relevant receding contact angles.

⁶ Here the effect that the droplets redistribute the axial momentum in the cross-section of the pipe is not considered. Redistribution of momentum: droplets are accelerating ('absorbing' momentum) upon moving to high gas-velocity regions (core) and decelerate ('releasing' momentum) upon moving to low gas-velocity regions (wall).

⁷ <http://www.kruss.de/services/education-theory/glossary/dynamic-contact-angle/>

⁸ This has been observed in previous projects to occur for low gas flow rates and not for high gas flow rates. As a result the minimum in the TPC is 'shifted' to lower gas flow rates.

4 Material selection and application

The materials that are selected to be tested in the large scale flow setup need to meet several criteria. It should be possible to apply the hydrophobic materials as coatings. The coating materials are preferably transparent (not a must) to be able to judge the flow profile by sight independent of the measurements. The coatings should be compatible with the test-tubes material and geometry for which PMMA has been selected due to its availability and optical transparency. Furthermore materials should be compatible with test conditions (no reaction with water, no swelling, no leaching of components, no side effects that may affect the setup or measurement equipment in any way). Materials that are not realistic to apply in view of price, availability, stability or toxicity should not be considered.

4.1 Classes of hydrophobic materials

Various chemical classes of hydrophobic materials exist. They have in common that a droplet of water (in equilibrium) on their (flat) surface displays a contact angle above 90°C . The observed contact angle is a result of a force balance between the surface energy of the (wet and dry) substrate and the surface tension of the droplet (water). The high contact angle of hydrophobic materials is explained by their low surface energy. The categories of materials that are relevant to the project –in increasing order of hydrophobic character- are briefly described below.

Hydrophilic – Most ceramics, most metals and some polymers (hydrogels, biopolymers) show hydrophilic behaviour (contact angle below 90°C). While most of the gas wells are constructed from uncoated stainless steel it should be considered that even the uncoated PMMA is much more hydrophobic compared to the situation in currently operating fields. The contact angle of steel surfaces can vary from complete wetting 0° to 60° or even higher depending on the oxidation state and adsorbing contaminations (gas condensates).

Epoxy Coatings – A minority of the gas wells have been coated to reduce corrosion or to reduce the friction (single phase flow). To this extent, epoxy and phenolic resin based coatings have been used. Tuboscope applies such coatings on the interior of steel pipes. The coating systems have in common that they contain highly reactive groups that can crosslink forming a dense thermoset polymer network. Low viscosity components are mixed and applied as a liquid or alternatively in the form of a powder coating. For improved mechanical performance, coatings are often cured at high temperature (up to 200°C), but room temperature cured systems (with or without catalyst) are known as well. High strength, hard, wear resistant, chemically inert protective coatings can be formed but they are typically not hydrophobic by themselves. The reactive groups are rather polar and leave hydroxyl groups when they have reacted. The hydroxyl groups are also polar and that attract water which can cause an overall hydrophilic behaviour. Commercially available additives, surfactants or waxes can be used to make epoxy coatings hydrophobic. BYK is a supplier of such additives.

Polyurethane coatings – Another class of commonly used high performance coatings (automotive, construction). Dense polymeric thermoset networks can be

formed from 2-pack polyurethane formulations. Compared to epoxies, polyurethanes are usually more tough or flexible rather than hard and rigid. High conversions can be reached at low temperatures. Depending on the exact chemical composition polyurethanes can be hydrophilic or hydrophobic. Additives can be used to modify the wetting properties.

Poly-methylmethacrylate (PMMA) – The acrylate groups are somewhat polar but the remainder of molecular structure is non-polar, making the material overall slightly hydrophobic. The wetting of PMMA is not representative for steel gas wells, but the material is optically transparent and therefore preferred for the large scale flow setup in this project. PMMA tubes have been coated with various coatings that are either more hydrophobic than PMMA itself or interesting as a reference (comparison to hydrophilic steel or commercially used coatings).

Poly-olefins – Polyethylene and polypropylene. Although they are widely applied (possibly the most applied) polymers that are hydrophobic, they have not been included in the project for practical reasons. Transport tubes of poly-olefins often contain non-transparent fillers. Furthermore, the polymers cannot be applied as a coating from a fluid because they are insoluble in any solvent (at room temperature). These thermoplastic polymers could be applied from a polymer melt, but it would be complicated to do that on the interior of a PMMA tube. Polyolefines melt at elevated temperature (~120°C for PE and somewhat higher for PP) and need dedicated polymer processing equipment (extruder, injection moulding etc.) to be applied on a surface.

Chlorinated polymers – The most common type in this class is poly-vinyl chloride PVC. PVC itself is not included in the project due to the same practical reasons as stated in case of poly-olefins (cannot be applied from polymer solution, neither from polymer melt). Low molecular weight analogues however can be used as a model component. Such smaller molecules can be dissolved in a solvent. The polymeric solution can be applied on the interior of the tube and the wetting behaviour should be representative for other chlorinated polymers like PVC.

Silicone based materials – this class includes soft materials like hydrophobic silicone rubbers as well as some glassy hydrophobic sol-gel systems (and many others in between). The expected hydrophobic behaviour is comparable to the chlorinated systems. Coatings are commercially available that can readily be applied from a solution or they are applied as liquid monomers/oligomers that are cured at elevated temperature or upon UV-light exposure. In this project a commercially available UV-curable hard-coat of high wear resistance has been included in the tests.

Fluorinated Polymers – Fluorinated materials display the strongest hydrophobic behaviour but are also difficult to process. The best known example is polytetrafluorethylene (PTFE or known as Teflon). PTFE cannot be applied from solution or from a polymer melt (it decomposes directly after melting which requires a very high temperature). TNO developed an alternative coating consisting of a poly-acrylate backbone having fluorinated pendant side-chains. The backbone allows the material to be applied from a solvent (although only heavily fluorinated solvents can be used) and to adhere to the substrate. The pendant side-chains of

the coating that are directed away from the substrate cause the characteristic hydrophobic behaviour.

4.2 Coatings based on hydrophobic materials

Besides influencing the contact angles, other material properties are associated to the surface energy as well. Materials that contain only surface energy groups tend to be soft, chemically inert (and therefore in some cases bio persistent), insoluble in commonly used solvents and difficult to adhere to other materials. For many applications (for example protection in extreme environments, friction reduction or improved release) such properties are desired, but to make coatings from them is a challenge. The high stability chemical inertness on one hand makes it difficult to formulate two-pack coatings (like conventional epoxy or polyurethane systems that are of high reactivity). The poor solubility in solvents on the other hand makes it difficult to formulate coatings that can be applied from a polymer solution. Furthermore additional effort may be required to improve the adhesion of hydrophobic coatings and the sensitivity towards (abrasive) wear. Depending on the application such difficulties are typically solved by either choosing a material that is a bit less hydrophobic (if possible) or by embedding other functional groups to accommodate for chemical crosslinking, substrate anchoring or solubility enhancement.

4.3 Boundary conditions for application of coatings on PMMA substrates

When using PMMA as a substrate material for coatings, several aspects relating to the specific chemical and mechanical properties of PMMA need to be taken into account.

4.3.1 *Stress corrosion*

PMMA is stress corrosive for certain commonly used solvents including alcohols like isopropanol. After mechanical processing of the material, remaining stresses are to be released. An annealing procedure is followed where the material is heated well above the glass transition temperature followed by a slow and gradual cooling. Due to the extrusion and fabrication processes, stress levels of polymer tubes may be substantially higher compared to flat test-substrates. This should be taken into account when comparing a coating applied on the interior of a tube to the same coating applied on a flat panel.

4.3.2 *Solubility and solvent swelling of PMMA*

The interaction between PMMA and the solvent of the coating is critical. If the solvent is too polar (like water), it will not wet the substrate well. Dewetting takes place, causing irregular coating deposition. If the interaction between PMMA and the solvent molecules is too strong the tubes dissolve in the coating, which should also be avoided. Strong solvents can negatively affect the mechanics and optical transparency of the tubes and contaminate the coating. A moderate interaction between solvent and polymer cannot cause the material to dissolve, but may to some extent swell the material at the surface. Swelling of the PMMA can be beneficial as some of the coating material can enter the swollen layer. Upon drying

of the system the coating remains mechanically anchored causing and improved adhesion.

4.3.3 *Curing a coating on PMMA*

For thermally curing of a coating on a PMMA substrate the temperature should not exceed the glass transition temperature too much (105 °C) for a long time as deformation of the tubes may take place. Short term heat exposure should always remain well below the melting point of PMMA (160 °C). Apart from glass transition and melting points the thermal expansion coefficient should be considered. If the coating expands/shrinks much more compared to the PMMA substrate with respect to changing temperatures cracking and delamination of the coating can be caused. The effect is closely related to the coating flexibility, yield strength and layer thickness. In some cases (brittle coatings) we had to reduce the layer thickness of the coating to stay below the delamination threshold.

4.3.4 *Flow coating of tubes interior*

As it is the inner surface of the tubes that needs to be coated, many conventional coating application procedures are excluded. There is no space for brush coating, powder coating or spraying. The only remaining option is flow coating where a curtain of fluid coating material is flown over the surface of the tube. To get a homogeneous coating layer of the desired thickness, the amount and type of solvent needs to be optimized. Solvents that are used for dilution need to be well miscible with the coating fluid and compatible with PMMA. Furthermore, if the viscosity is too high, the flow pattern becomes irregular. If the viscosity is too low, too little material remains immobilized on the surface. The solvent should not evaporate too fast (causing the coating to become solid before the surface is well covered), but also not too slow, to prevent the coating from sliding to the bottom of the tube after it has been applied.

In summary coating materials have been selected according to two major criteria:

- Keep a *high degree of diversity* in the coating selection in terms of chemistry and in terms of the different classes of hydrophobic materials. A substantial contrast between the materials is preferred when relating their flow properties to the coating properties.
- Selected materials should meet the *processing boundary conditions* meaning it should be possible to make a coating from the material and that the coating should be compatible with the PMMA substrate. Furthermore it should be feasible to apply the coating on the interior of narrow tubes.

4.4 **Application procedures for selected coatings**

Selected materials range from strongly hydrophobic systems that are not widely applied in the oil- and gas industry (fluorinated, chlorinated or silicone based), to commercially available coatings that have been applied on currently operating gaswells (epoxy) and a few systems in between (alternative epoxy with and without functional additives). The coatings are synthesized and formulated by TNO or commercially available systems, where in most cases the formulation or coating application procedure has been adjusted. Below selected systems and optimized

application procedures are discussed in detail including the preparation and cleaning of the substrates.

Substrate preparation – flat PMMA substrates are cut into 50 mm x 50 mm test panels. The protective foil is removed and the substrates are washed with water and soap. The last traces of impurities are removed using a UV ozone treatment which also activates the surface to improve the adhesion. Deionized air could be used to neutralize statically charged locations that can interfere with contact angle measurements. PMMA tubes are cut at length and holes are drilled to accommodate for water injection and mounting of pressure sensors. After machining of the tubes, stresses are released by the thermal annealing method. Subsequently the tubes have been cleaned using water and soap after which they are dried in the oven.

Fluorinated Coating – A fluorinated acrylic monomer is diluted (1:1) in a fluorinated solvent. A thermal initiator (1% w/w with respect to monomers) is added to the mixture and the polymerization is carried out at elevated temperature in an inert N₂ atmosphere. After 16 hours the coating fluid is obtained by further dilution of the polymer solution with fluorinated solvent (until 1% w/w). Prior to use, the coating fluid is filtered. The polymer solution is flow-coated over the surface of the substrate and the solvent is evaporated in the oven (4 hours at 70°C).

Chlorinated Coating – A chlorinated rubber is dissolved in a solvent mixture containing predominantly xylene to achieve the desired viscosity. The polymer solution is applied on the surface of the tubes by means of flow coating. The solvent is removed through evaporation which is enhanced by applying heat in an oven.

Silicone based Coating – A commercial silicone hardcoat is used (AY 42-260, Dow). As solvents the product contains mainly isopropanol (~30%) and some toluene (~10%). Prior to use the product is filtered and further diluted with toluene (1:1). The solution is applied using flow-coating. The majority of the solvent is evaporated at ambient conditions, while rotating the coated substrates (in case of tubes) for 5 to 10 minutes to keep the film thickness homogeneous. A subsequent drying step is performed in the oven to immobilize the coating material on the substrate. The coating is subsequently cured using a UV source. PMMA is not transparent enough with respect to UV light meaning that curing can not be established by using an external light source. A setup is constructed to guide a UV conducting fibre through the tube interior for direct exposure of the coated surface. The fibre is gradually moved (several minutes per section) in the direction of the curing to avoid a contact between the UV-fibre and uncured (soft) coating material on the wall. Upon curing a nitrogen flow is applied through the tube to lower the concentration of oxygen which acts as a polymerization inhibitor.

PUR – A commercially available two component PUR (anti-graffiti coating, TEMAC) is used. Both components are mixed (in a 2 to 1 ratio as advised by the supplier) and diluted in brush thinner (P101). The fluid is applied on the surface using flow coating. The solvent is evaporated at ambient conditions (tubes are rotated upon drying).

Model Epoxy with and without additives – Diethylenetriamine, DETA, is added to the diglycidyl ether of bisphenol-A, DGEBA (12 gram per 100 gram). The mixture is

vigorously stirred and diluted with toluene. Optionally max. 5% (w/w with respect to the total mass of solids) of a commercial additive (BYK-605) is added to enhance the hydrophobic behaviour. The resulting coating fluid with or without additive is applied using flow coating directly after preparation. The solvent is left to evaporate at ambient conditions (while rotating the substrate). The coating is post cured in an oven.

Tuboscope reference coatings – Coatings are applied by tuboscope (epoxy or phenolic based systems). Coatings are applied on steel according to their procedures (sanding, priming, powdercoating) and cured at high temperature to obtain rigid coatings of high glass transition temperature.

Other materials – many other coatings have been explored in an early stage of the project. They did not qualify for the selection due to various reasons. Some strongly hydrophobic materials that are commonly used on textiles could not be made compatible with PMMA substrates due to wetting issues of the coating fluid, its pH and advised curing temperature. Some commercially available hydrophobic waxes or fluorinated surfactants could not be immobilized on the PMMA surfaces as they remained water soluble after application or crystallize into inhomogeneous layers.

Several experiments have been conducted on rough carrier substrates as it is well known that a combination of micro- and nano-roughness may tremendously enhance the hydrophobic behaviour. Porous rigid polymer foam, glass fibre filter and filter paper have been explored as rough coating carriers for amplification of the hydrophobic behaviour, but they were found unsuccessful, or, in case of the foam not useful as it is too complex to apply a layer of foam in the interior of a tube.

5 Coating Analysis

Wetting phenomena taking place on various scales are measured and related. Contact angle analysis gives quantitative information about the top 1 nm of a surface, while the impact test (more qualitative by nature) shows the behaviour of droplets impacting on a surface (typically ~1cm scale effect). The full scale flow tests are performed to quantify wetting effects taking place on the scale of a few meters and beyond.

5.1 Contact angle measurements

5.1.1 *Relevance of Dynamic Contact angle Measurements*

The most conventional type of contact angle measurements is the static contact angle. In this case a small droplet (small enough to allow for ignoring of gravitational forces) of a well-defined fluid (usually water of high purity) is applied on a substrate. An automated goniometer can be used for controlled delivery of the droplet and the integrated camera and software provide the angle between the droplet and substrate at rest which referred to as the static contact angle. In our case we use a goniometer to determine the dynamic contact angles, that are of much more importance compared to static contact angle as we aim to relate the wetting properties to flow regimes that are by definition non static. The behaviour of a droplet moving with respect to a surface (droplet sliding over a surfaces or a droplet expanding on a fresh surface or a droplet withdrawing from a wetted area) is characterized by the advancing contact angle (the maximum contact angle) and the receding contact angle (minimum contact angle). The advancing contact angle is typically (somewhat) larger compared to the static contact angle and the receding contact angle may be somewhat smaller or much smaller compared to the static contact angle depending on factors including coating homogeneity, presence of pinholes and surface topology. In some cases it is possible that a droplet flows poorly over a strongly hydrophobic surface (i.e. static contact angle $\gg 90^\circ$), if that surface has a very low receding contact angle (due to local defects or trapped charges or the like). In some other cases a droplet may flow very well over a hydrophilic surface if the hysteresis (dynamic contact angle minus receding contact angle) is low. Small defects in the surfaces or local variation in the wetting properties (like pinholes) can be a cause of such hysteresis.

5.1.2 *Measurement protocol*

A Krüss DSA100 goniometer is used to apply droplets of milli-Q water having a resistivity as high as 18.2 MΩcm. A automated droplet expansion retraction cycle is followed while the contact angles are being measured every second. A small droplet (<1 μL) is deposited and the volume is gradually increased (10μL/min) until a volume well above 10μL is reached. As the droplets increases and the wetted area is expanding a saturation plateau may be observed in the contact angle profile which is referred to as the advancing contact angle. After the expansion phase the system is kept at rest for 0.5 minutes during which the volume may slightly decrease due to evaporation. In the subsequent phase liquid is withdrawn from the droplet through the needle with a constant velocity of 10 μL/min. While the droplet shrinks it changes its shape (becomes flatter) while the total wetted are remains unchanged. At a certain stage the shrinking droplet keeps its shape but continues

to shrink. When that happens the wetted area is reduced and the contact angle reaches another plateau which is referred to as the receding contact angle. The lower the receding contact angle, the more difficult it becomes to measure it with high precision. Below 1 to 3 μL the measurement was stopped. A low receding contact angle means the droplet is flat (it becomes more difficult to collect the remaining fluid with the needle) and it hardly has any volume (error in the measured volumes becomes relatively large) explaining the increased noise levels observed for measurements on systems that are not strongly hydrophobic. If the receding contact angle is too low it cannot be measured.

5.2 Impinging droplet tests

During the impingement droplet tests, droplets are released a distance l above a flat horizontal surface. The distance l has varied from 2.5 to 12 cm, resulting in an impinging velocity ranging from 0.7 to 1.5 m/s (assuming a constant acceleration of 9.81 m/s^2 and a zero release velocity). The released droplets have a diameter of about 5.2 mm. The process of impingement has been recorded using a high speed camera (Olympus i-speed 2, 800x600pcs) at a frame rate of 1,000 fps.

The results with droplets released at a height of $l = 6 \text{ cm}$ (i.e. an impingement velocity of $\sim 1.1 \text{ m/s}$), turned out to have the best image quality, and are therefore selected for intercomparing the coatings. The following surfaces have been subjected to the impingement tests:

- A. Cleaned PMMA
- B. Fluorinated coating on PMMA
- C. Contaminated Fluorinated coating on PMMA
- D. Fluorinated coating on a porous rigid polymer foam.
- E. Silicone based coating on PMMA
- F. Chlorinated coating on PMMA
- G. Model Epoxy with BYK-605 on PMMA
- H. Tuboscope reference coating on RVS

Ad C.) The contamination has been achieved by wetting a clean Fluorinated coating using tap water and letting the water evaporate in the air (i.e. leaving traces of minerals). This process has been repeated several times.

The elasticity of the droplet rebound is determined by measuring the maximum height the droplet (or its satellite) will reach upon rebound. With a perfect elastic rebound the droplets could reach their initial release height approximately.

5.3 Flow loop tests

During the flow loop tests the effect of coatings applied on the pipe wall have been studied. The flow loop is a vertical acrylic (PMMA) pipe with an ID of 20 mm and a length of 3 m. The loop is built from 10 segments (each 0.3 m long) to facilitate the coating process. Since the coating needs curing at elevated temperatures, the PVC connections have been glued to the PMMA pipe segments after coating has been applied. The following surfaces have been subjected to the flow loop tests:

- A. Cleaned PMMA
- B. Fluorinated coating on PMMA
- C. Contaminated Fluorinated coating on PMMA
- E. Silicone based coating on PMMA
- G. Model Epoxy with BYK-605 on PMMA

Dry air is injected at the bottom of the pipe and is mass-flow controlled using a Bronkhorst controller (Bronkhorst IN-FLOW F-206AI-RAD-44-V, maximum capacity: $38.3 \cdot 10^{-3} \text{ Nm}^3/\text{s}$, accuracy: 0.2% FS). The superficial gas velocity during the tests ranged from $U_{\text{sg}} = 2 - 40 \text{ m/s}$ (i.e. $0.6 - 12.6 \cdot 10^{-3} \text{ Nm}^3/\text{s}$).

Tap water is injected at $\sim 17D$ above the gas inlet via 4 small ID holes (i.e. similar to design I of Khosla, see section 2.3) and is mass-flow controlled using a Bronkhorst controller (Bronkhorst M15-RAD-44-0-s CORI-FLOW, maximum capacity: $62.8 \cdot 10^{-3} \text{ kg/s}$, accuracy: 0.1%). The superficial liquid velocity in the tests is taken $U_{\text{sl}} = 0, 3, 10$ and 30 mm/s (i.e. maximum $9.4 \cdot 10^{-3} \text{ kg/s}$). This results in a maximum LGR of $\sim 2300 \cdot 10^{-6} \text{ m}^3/\text{Sm}^3$ at the minimum in the TPC curve (i.e. $U_{\text{sg}} = \sim 13 \text{ m/s}$).

Figure 5.1 shows the gas inlet and liquid inlet of the flow loop.



Figure 5.1 Left: Gas inlet and liquid inlet of the flow loop set up. The capacitance probes are mounted on the first segment. Right: top half of the flow loop connected downstream to the atmospheric air/water separator.

At the outflow of the setup a separator is located: the air is released to the atmosphere and the water is drained to the sink. The flow loop is kept at atmospheric conditions.

The pressure gradient has been measured at two locations:

1. Between 107D and 137D from the gas inlet, using dp sensor 1 (Rosemount 1151 HP4 F22/8, range 0-100mbar, accuracy: 0.1% FS, dx = 0.6m).
2. Between 92D and 137D from the gas inlet using dp sensor 2 (Yokogawa EJX110A, range 0-100mbar, dx = 0.9m).

Both dp-sensors are located at the level of the gas inlet. The tubing from the sensors to the pressure connections at the flow loop has been filled with water. During the experiments it has been checked that air-bubbles are not present in the connection lines.

Capacitance probes are used to detect the presence of water and, if possible, to assess the liquid holdup. The capacitance probes are TNO design and consist of two copper plates (~1x2cm) wrapped around the tubing at opposite positions (see also Figure 5.1). The capacitance between these copper plates is measured and depends on the amount of liquid present in the tube near these copper plates. Here, the capacitance probes are used only to detect the presence of water below the liquid injection (i.e. the onset of liquid loading). Calibration is not needed to detect the presence of water.

A webcam (Microsoft Lifecam Cinema, 10 fps) has been used to record images of the flow pattern at the top segment.

Data acquisition has been done using a Dewetron (DEWE-801) at a sampling frequency of 1 kHz.

In the laboratory setup described above, the liquid loading point is defined as the gas flow rate at which some liquid start to appear upstream of the liquid injection upon decreasing the gas flow rate from an initial concurrent annular/droplet flow.

6 Results and Discussion

6.1 Contact angle measurements

The dynamic contact angle curves obtained with increasing and subsequent decreasing droplet volume are displayed in Figure 6.1 and Figure 6.2. The measurements are recorded in duplo or triplo to give an idea about the reproducibility of the obtained values. Where possible the plateau values of those graphs are compared in Figure 6.3. In the first stage of the measurement (upper curves from left to right) advancing contact angles are measured while a droplets is expanding in volume over a fresh surface up to $> 12 \mu\text{L}$ corresponding to $\sim 3\text{mm}$ size droplets after which the flow is reversed (2nd stage : lower curves from right to left) to determine the receding contact angle from a droplet while it is receding from a wetted surface.

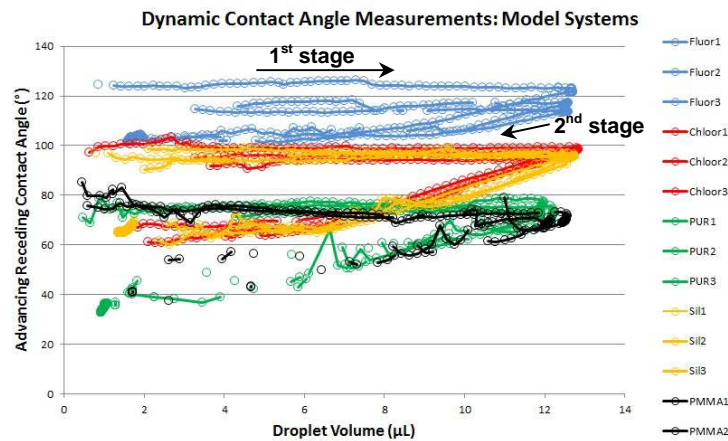


Figure 6.1 Overview of wetting behaviour of coated surfaces.

As expected the most hydrophobic system is the fluorinated coating. Even when the droplet volume is reduced to determine the receding contact angle, the plateau remains well above 100° . The fluorinated system is followed by the chlorinated rubber and the silicone based hardcoat that show more or less de same wetting behaviour. It was therefore decided not to include the chlorinated rubber in the large scale flow test.

The poly urethane and the PMMA are less hydrophobic compared to the chlorinated coating, the silicone based system and the fluorinated acrylate. Although the curves of the polyurethane and the PMMA are in the same range of contact angles, a clear plateau formation for the receding contact is clearly observed in case of the poly urethane. In case PMMA however, when the droplet volume is decreased below $\sim 7 \mu\text{m}$ the noise becomes very large causing discontinuities in the curve and a clear plateau formation is not observed. If the receding contact angle is very low (much lower compared to the advancing contact angle) droplets of water may not flow easily over such a surface. In case of PMMA this may be caused by pinning due to impurities or inhomogeneity in the surface topology or composition.

Conventional epoxy systems are typically not applied as strictly hydrophobic coatings but they are included in the study because some gas wells are coated with an epoxy for improved flow insurance (usually through friction reduction). The model epoxy that should be well comparable to coatings that are being used in the field in terms of surface chemistry and texture resembles the wetting behaviour of the PMMA. The measured contact angles are within the same range of $\sim 40^\circ$ to $\sim 80^\circ$ and we see again the discontinuity at lower volumes (i.e. absence of a receding contact angle plateau).

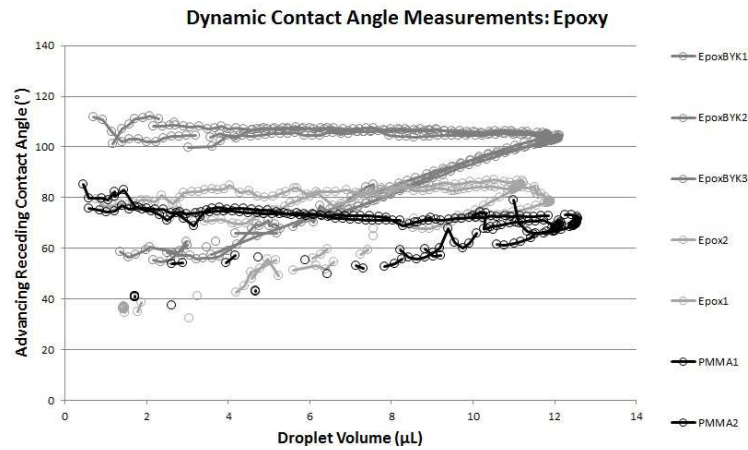


Figure 6.2 Dynamic contact angle measurements of epoxy based systems with and without hydrophobic additive in comparison to the substrate material (PMMA).

A commercially available additive was used to see to what extent the properties of a common epoxy coating could be boosted to bridge the gap to the more hydrophobic behaviour of the silicone, chlorinated and fluorinated coatings. It was observed that addition of a BYK additive not only caused an increase of the contact angles throughout the entire measurement range (with increasing droplet volume as well as decreasing droplet volume) but also gave rise to a very clear plateau formation with associated receding contact angle of 57° .

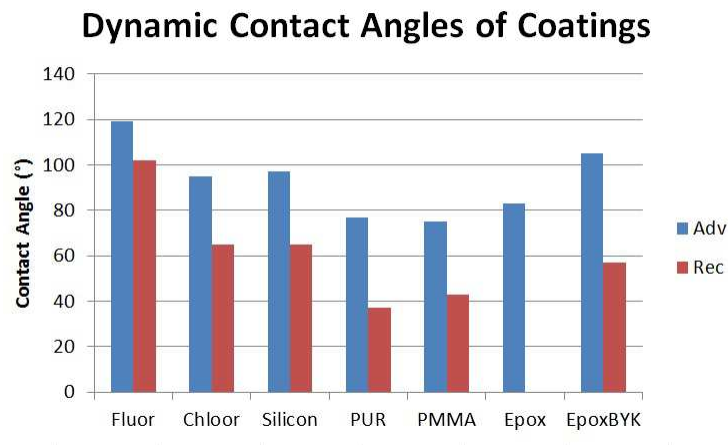


Figure 6.3 Advancing and receding contact angles obtained from plateau values in Figure 6.1 and Figure 6.2.

6.2 Droplet impingement tests

Upon release of a droplet from the syringe, it accelerates and impacts with the surface. The water droplets (~5.2mm diameter) are released from a height of 6 cm, hence impact with a velocity of about 1.1 m/s. Upon impact, the droplets spread out on the surface in the form of a disc with a thick rim. Hereafter, the droplet retracts and possibly (partially) detaches from the surface.

Figure 6.4 to Figure 6.6 show snapshots of the process of droplet impingement onto various surfaces, and Table 6.1 lists the rebound height of the water droplets for all tested surfaces.



Figure 6.4 Droplet impinging on PMMA substrate (A). Left: just before impact, center: maximum wetting of the surface, right: maximum height of retracted droplet.

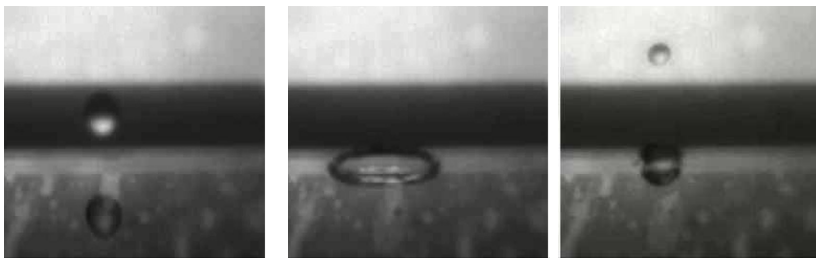


Figure 6.5 Droplet impinging on Fluorinated coating on PMMA (B). Left: just before impact, center: maximum wetting of the surface, right: maximum height that a satellite obtains.

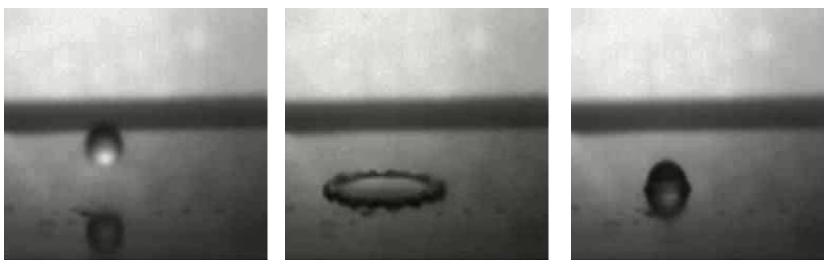


Figure 6.6 Droplet impinging on Chlorinated coating on PMMA (F). Left: just before impact, center: maximum wetting of the surface, right: maximum height of retracted droplet.

From all impingement tests, only substrate B (i.e. Fluorinated coating on PMMA) shows a partial detachment of liquid after impact. All other substrates show a rebound of the droplets that is only slightly higher than the steady state end situation (i.e. with the droplet lying in rest on the surface). A remarkable result, is that the 'contaminated' Fluorinated surface (substrate C) showed rather a poor droplet reboundability, even though the surface still seemed hydrophobic. Possibly, this is related to pinholes emerging on the surface.

Table 6.1 Dynamic contact angles (section 6.1) and droplet rebound height for 5.2mm diameter water droplets released 6 cm above a flat coated substrate.

ID	Surface	CA _{adv} (°)	CA _{rec} (°)	Rebound height (mm)
A	Cleaned PMMA	75	43	2.1
B	Fluorinated coating on PMMA	119	102	15.6
C	Contaminated Fluorinated coating on PMMA	91*	73*	2.1
D	Fluorinated coating on a porous rigid polymer foam	139	139	4.2
E	Silicone based coating on PMMA	97	65	4.2
F	Clorinated coating on PMMA	95	65	3.6
G	Model Epoxy with BYK-605 on PMMA	105	57	2.6
H	Tuboscope			2.1

* The contact angle estimate with the contaminated Fluorinated coating has not been performed using the protocol described in section 5.1, but has been estimated by measuring the contact angle of a droplet attached on the inner wall of a pipe, rotated on its axis until the droplet starts sliding downward (but maximum by 90°), see Figure 6.12.

Chen et al. (ref. 2) also mention the effect of pinholes on droplets impinging on flat surfaces. They observe that for large impact velocities (1 - 2 m/s), droplets are pinned to hydrophobic surfaces⁽⁹⁾ in the retracting phase. They explain this by the wetting pressure exceeding the anti-wetting pressure⁽¹⁰⁾. When the wetting pressures are larger than the anti-wetting pressures, the droplets penetrate in the roughness structure which pins the droplets to the surface.

Note that the impingement test is a different process is than the dynamic contact angle measurements, and thus may give different results: a Fluorinated coating on a porous rigid polymer foam gives very high contact angles, but does not show a good reboundability.

Conclusions

From the impingement tests it is concluded that a high receding contact angle correlates well with a good reboundability of droplets (hypothesis I). However, surface roughness seems to deteriorate this effect due to pinning of the droplets.

⁹ Chen et al. tested superhydrophobic surfaces that are created by micro-roughness: natural occurring on lotus leaves and artificial created using carbon nano-tubes deposited on a silicon substrate.

¹⁰ The wetting pressure is the waterhammer pressure plus the dynamic pressure, and the anti-wetting pressure is the capillary pressure caused by the air trapped by the surface roughness.

6.3 Flow loop tests

6.3.1 Substrate A: cleaned PMMA

Figure 6.7 shows the flow patterns observed during the tests for the PMMA pipes (substrate A). The flow patterns are churn-annular flow for $U_{sg} < \sim 10$ m/s and annular flow for $U_{sg} > \sim 10$ m/s. (note that this is not very clearly visible in Figure 6.7).

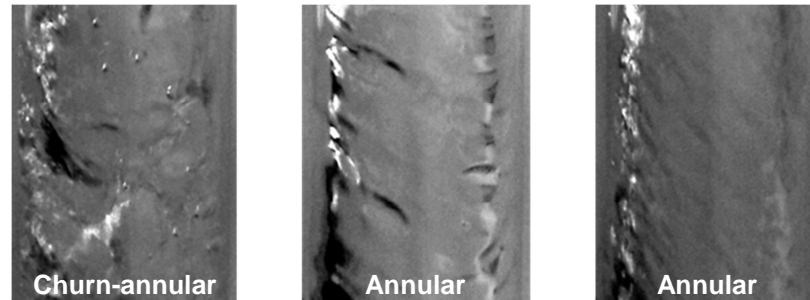


Figure 6.7 Video stills taken from the outside of the flow in clean PMMA pipes with (from left to right) $U_{sg} = 4, 14$ and 30 m/s and $U_{sl} = 10$ mm/s.

Figure 6.8 shows the TPC curves measured for the PMMA pipes for various values of the liquid flow rate. For the flow conditions indicated by the filled triangles, the capacitance probes indicate the presence of liquid below the injection, for the open symbols there is no liquid present below the injection. The results of the MSc thesis of Khosla are shown as well, indicating a reasonable level of reproducibility with respect to the pressure gradient and the onset of liquid loading (dashed line).

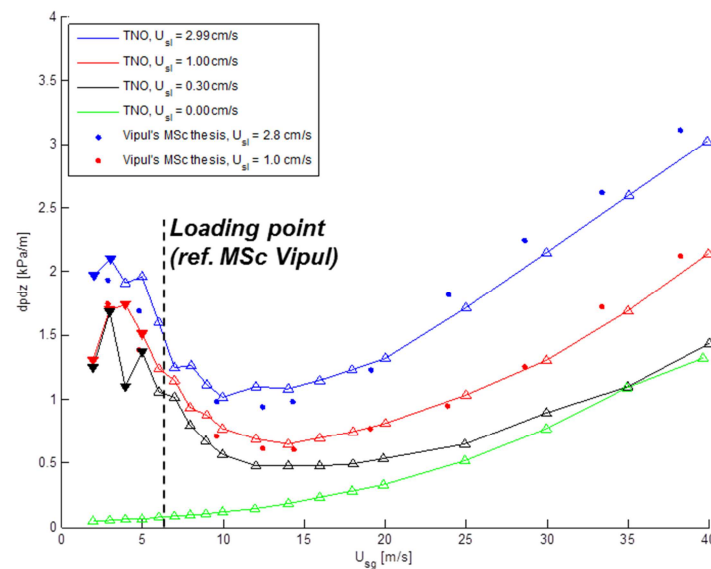


Figure 6.8 TPC curves for the PMMA pipes (substrate A) for various values of the liquid flow rate. The results of the MSc thesis of Khosla are shown as well.

The minimum in the TPC curve varies slightly with liquid flow rate around $U_{sg} = 13$ m/s (i.e. $F_g = U_{sg} \sqrt{(gD) \sqrt{(\rho_g/\Delta\rho)}} = \sim 1$), and the onset of liquid loading lies near $U_{sg} = \sim 4$ m/s. The pressure gradient at the minimum in the TPC for $U_{sl} = 10$ mm/s is

~ 650 Pa/m. The curve with $U_{sl} = 0$ is used to estimate the hydraulic roughness and gives $k_s = \sim 35$ μm .

6.3.2 Substrate B: Fluorinated coating on PMMA

Figure 6.9 shows the flow patterns observed during the tests for the Fluorinated coated PMMA pipes (substrate B). The flow patterns are inverted-churn flow for $U_{sg} < \sim 10$ m/s and droplet flow for $U_{sg} > \sim 10$ m/s (note that this is not very clearly visible in Figure 6.9).

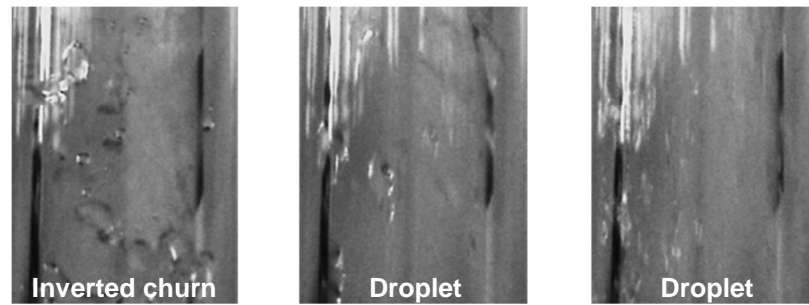


Figure 6.9 Video stills taken from the outside of the flow in Fluorinated coated PMMA pipes with (from left to right) $U_{sg} = 4, 14$ and 30 m/s and $U_{sl} = 10$ mm/s.

Figure 6.10 shows the TPC curves measured for the Fluorinated coated PMMA pipes for various values of the liquid flow rate. For the flow conditions indicated by the filled triangles, the capacitance probes indicate the presence of liquid below the injection, for the open symbols there is no liquid present below the injection. The results of the MSc thesis of Khosla are shown as well indicating again a reasonable level of reproducibility with respect to the pressure gradient and the onset of liquid loading (dashed line).

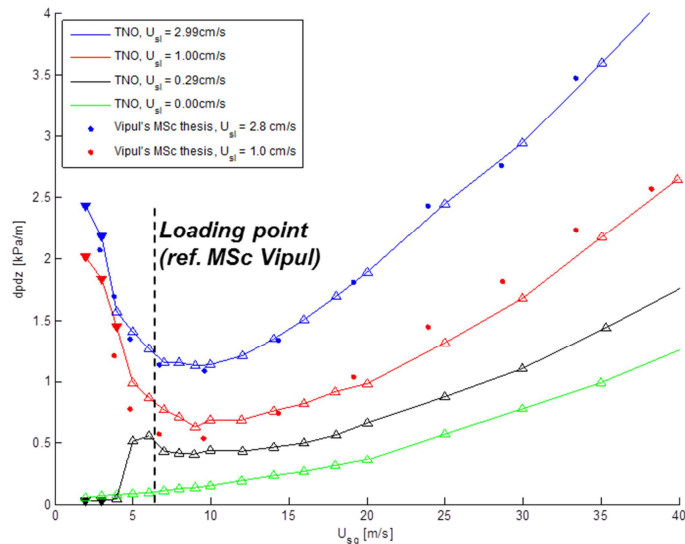


Figure 6.10 TPC curves for the Fluorinated-coated PMMA pipes (substrate B) for various values of the liquid flow rate. The results of the MSc thesis of Khosla are shown as well.

The minimum in the TPC curve varies slightly with liquid flow rate around $U_{sg} = 9$ m/s (i.e. $F_g = \sim 0.7$), and the onset of liquid loading lies near $U_{sg} = \sim 4$ m/s. The pressure gradient at the minimum in the TPC for $U_{sl} = 10$ mm/s is ~ 600 Pa/m. For gas flow rates between the onset of liquid loading and the minimum in the TPC curve, the pressure gradients are lower for the Fluorinated-coated PMMA than for the cleaned PMMA. This is beneficial for deliquification and has been observed in previous projects as well. The gas flow rate at the onset of liquid loading is not significantly affected by the coating.

The curve with $U_{sl} = 0$ is used to estimate the hydraulic roughness and gives $k_s = \sim 20$ μm , which is considered to be similar to the value for clean PMMA. From this it is concluded that the Fluorinated coating does not affect the hydraulic roughness.

6.3.3 Substrate C: Contaminated Fluorinated coating on PMMA

After testing for a few hours, the fluorinated-coated PMMA showed a remarkable and significant change in flow behaviour, probably caused by contamination. Since the flow behaviour differs much from the uncontaminated coating, it has been treated as a separate 'coating'.

Visually, the flow patterns remained unaffected, but the pressure gradients increased significantly for $U_{sg} < \sim 15$ m/s, while for $U_{sg} > \sim 15$ m/s the pressure gradients decreased. Figure 6.11 shows the TPC curves measured for the contaminated Fluorinated-coated PMMA pipes for various values of the liquid flow rate. For comparison, the results of the clean Fluorinated-coating from Figure 6.10 are replotted here as well (gray lines). For the flow conditions indicated by the filled triangles, the capacitance probes indicate the presence of liquid below the injection, for the open symbols there is no liquid present below the injection.

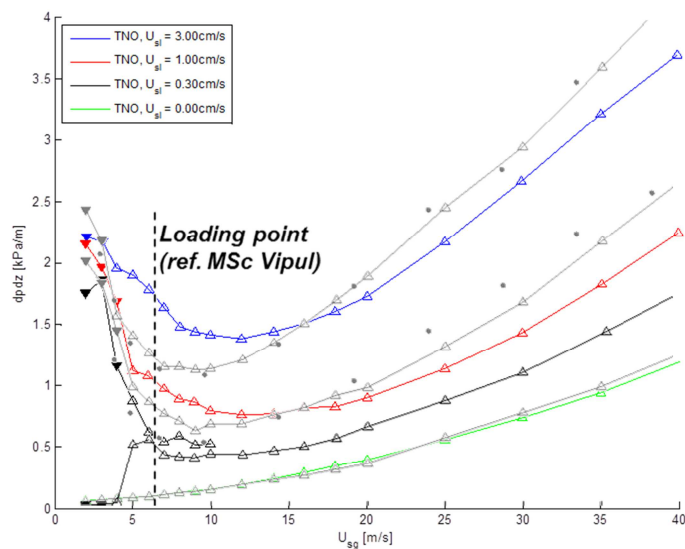


Figure 6.11 TPC curves for the contaminated Fluorinated-coated PMMA pipes (substrate C) for various values of the liquid flow rate. The results of the clean Fluorinated-coated PMMA are shown as well (gray lines).

The minimum in the TPC curve varies slightly with liquid flow rate around $U_{sg} = 13$ m/s (i.e. $F_g = \sim 1$), and the onset of liquid loading lies near $U_{sg} = \sim 4$ m/s. The pressure gradient at the minimum in the TPC for $U_{sl} = 10$ mm/s is ~ 725 Pa/m.

The contaminated Fluorinated-coated PMMA pipes even perform worse than the clean PMMA pipes: the minimum in the TPC curves are approximately equal to that of the clean PMMA pipes, but the pressure gradient is larger. This effect is most pronounced at higher U_{sl} .

The changes in the Fluorinated-coated PMMA have been further studied by putting a single droplet on the inner surface of a horizontal-laid single pipe segment, see Figure 6.12. Hereafter, this pipe segment has been rotated on its axis. For the spare Fluorinated-coated PMMA segment that was not built-in (i.e. not exposed to the flow), the droplet easily flows over the pipe inner surface and stays at the bottom, see Figure 6.12 left graph. However, for the segments that were exposed to the flow, the droplet sticks to the wall (possibly due to pinholes) and rotates with the pipe, see right graph of Figure 6.12. This test has been used to estimate roughly the dynamic contact angles of the contaminated Fluorinated-coated PMMA.

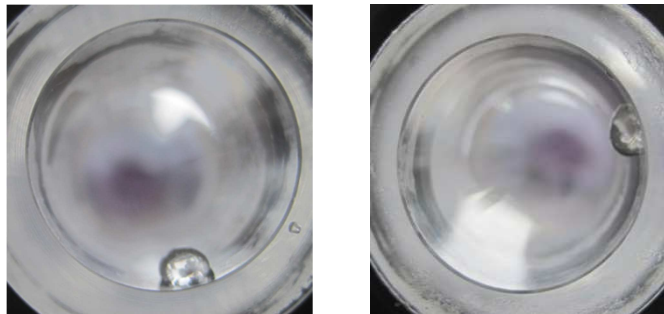


Figure 6.12 Left: single droplet laid on the inside of a spare Fluorinated-coated PMMA segment not exposed to flow. Right: single droplet laid on the inside of a Fluorinated-coated PMMA segment that is exposed to flow. The pipe segment is rotated on its axis, and the droplet sticks to the pipe wall and rotates along.

Cleaning the pipes using IPA showed a (partial) recovery of the initial hydrophobic properties. The contaminated pipe segments, that showed sticking of a droplet on the pipe wall upon rotating the pipe on its axis, did not show any significant sticking after this cleaning. From this, it is concluded that the coating is still intact and functioning, and that a small contamination layer (e.g. deposited minerals) had been deposited onto the Fluorinated-coating which can be removed by rinsing the inner surfaces.

The effect of minerals deposited on Fluorinated-coated PMMA have been studied also via the droplet impingement tests (see section 5.2 for the contaminating procedure). These tests showed a strong deterioration of the reboundability of droplets on a contaminated surface.

6.3.4 Substrate E: Silicone based coating on PMMA

The flow loop results of the Silicone based coating are very similar to those of the clean PMMA. Both the flow patterns and the TPC curves are alike.

Figure 6.13 shows the TPC curves measured for the Silicone base coating for various values of the liquid flow rate. For the flow conditions indicated by the filled triangles, the capacitance probes indicate the presence of liquid below the injection, for the open symbols there is no liquid present below the injection. For comparison, the results of the clean PMMA from Figure 6.8 are replotted here as well (gray lines).

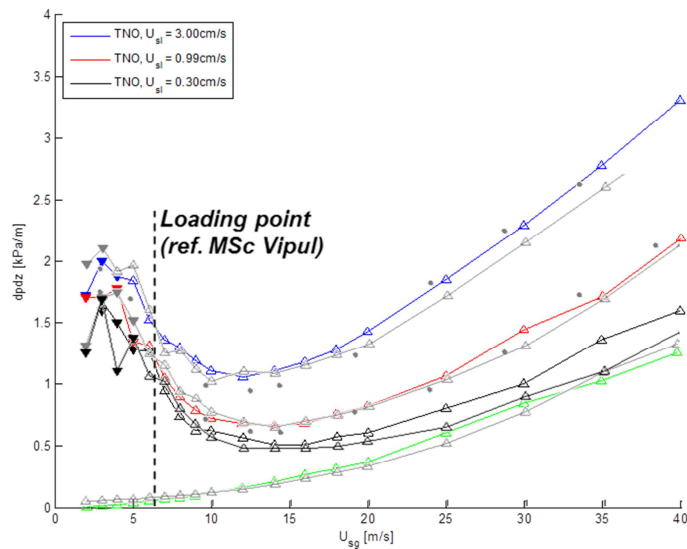


Figure 6.13 TPC curves for the Silicone based coating (substrate E) for various values of the liquid flow rate. The results of the clean PMMA are shown as well (gray lines).

6.3.5 Substrate G: Model Epoxy with BYK-605 on PMMA

The flow loop results of the Model Epoxy with BYK-605 are also very similar to those of the clean PMMA. Both the flow patterns and the TPC curves are alike.

6.3.6 Summary of flow loop tests

The results of the flow loop tests with respect to the flow patterns that are observed and the characteristics of the minimum in the TPC are summarised in Table 6.2. These results are also visualised in Figure 6.14 (red squares) together with the results from previous projects (blue diamonds, see chapter 2).

Table 6.2 Flow patterns and characteristic of minimum in TPC curve for $U_{sl} = 10$ mm/s.

ID	Surface	FP *	$U_{sg,min}$ (m/s)	$dpdx_{min}$ (Pa/m) **
A	Cleaned PMMA	C-AD	~13	650
B	Fluorinated coating on PMMA	IC-D	~9	600
C	Contaminated Fluorinated coating on PMMA	IC-D	~14	725
E	Silicone based coating on PMMA	C-AD	~14	670
G	Model Epoxy with BYK-605 on PMMA	C-AD	~14	650

* Flow pattern: C: churn flow, AD: annular dispersed, IC: inverted-churn, D: droplet flow.

** The minimum in the pressure gradient is given here for $U_{sl} = 10$ mm/s.

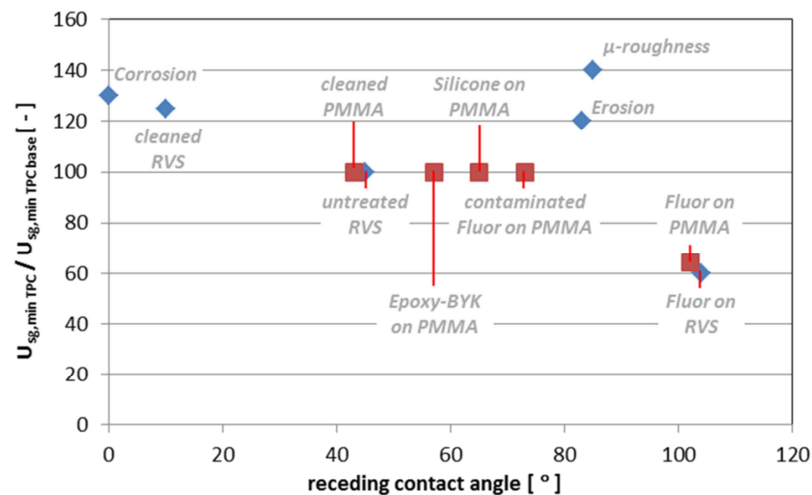


Figure 6.14 Performance ⁽¹¹⁾ of various coatings as a function of their receding contact angle. Red squares indicate results of this JIP, Blue diamonds represent results from previous projects.

Based on these results (and previous projects) the following is concluded:

- Several coatings have been tested in a flow loop. CA_{rec} of these coatings range from $\sim 55^\circ$ to $\sim 105^\circ$. The only coating that shows a positive effect (i.e. reduced pressure gradient for low gas flow rates) is the Fluorinated coating with $CA_{rec} = \sim 105^\circ$.
- A change in the flow patterns (i.e. from churn-annular to inverted-churn) does not necessarily result in a positive change in the TPC (i.e. reduced pressure gradient). Such a positive change was also not observed by Takamasa (2008).
- The use of tap water may indirectly affect the liquid loading behaviour by deposition of contaminants (e.g. minerals) on the coating from the water. This may have been the cause for the 'mis-functioning' of the Fluorinated-coating in the industrial scale of Game Changer III.
- Although roughness can enhance the hydrophobic properties of a coating, the dynamics upon droplet impact in flows can cause pinning, which counters the effects of hydrophobicity.
- The liquid loading behaviour for PMMA and clean Fluorinated-coating correspond well with results from previous projects (i.e. good reproducibility).
- The results of the flow loop tests correspond with the results of the impingement tests : the Fluorinated coating shows both a good reboundability as well as a significant reduction of the pressure gradient. This suggests that the impingement test can be a simple and quick method for assessing the functionality of the coating.

¹¹ The performance of a coating is defined as gas flow rate at the minimum in the TPC for that coating normalised by the gas flow rate at the minimum in the TPC for the 'base-case'. The base case is either PMMA or untreated RVS.

- The onset of liquid loading (i.e. the gas flow rate at which liquid appears below the liquid feed) is not significantly affected by a hydrophobic coating. This has been observed in previous projects as well.
- With respect to the posed hypotheses:
 - II. *Increasing the reboundability of droplets cause a change in flow patterns.*

This seems not completely true, since the contaminated Fluorinated coating shows poor reboundability, but still a change in flow patterns. The receding contact angle is second best for all surfaces tested, hence a better statement would be : a receding contact angle above $\sim 70^\circ$ is required to obtain inverted-churn flow.
 - III. *Under conditions of inverted-churn flow, a more elastic rebound of droplets reduces the pressure gradient.*

A reduction of the reboundability in the impingement test for the contaminated Fluorinated coating compared with the clean Fluorinated coating coincides with an increase of the pressure-gradient. It is noted here that the presence of an inverted-churn flow does not necessarily result in a reduced pressure gradient compared to a 'normal' churn flow.

7 Summary and Conclusions

7.1 Materials

A multitude of coatings have been explored and compared with the aim to delay the onset of liquid loading through modification of wetting behaviour based on which a fluorinated, chlorinated, silicone, polyurethane, PMMA and epoxy based systems were selected for further study. The dynamic contact angles of the selected materials have been measured on flat substrates, confirming that the wetting properties of the various classes of selected materials are well distributed over the range of interest. In case of the substrate material (PMMA) and the unmodified model epoxy (representative of coatings that are currently used by the oil- and gas industry) no clear receding contact angle was observed which inhibits the flow of droplets with respect to such surfaces. The absence of a receding contact angle plateau of the epoxy could be solved by using a commercially available additive. The additive also caused a large increase of the advancing contact angle well into the hydrophobic regime (up to 105°).

Based on the dynamic contact angle measurements, the PMMA, fluorinated, silicone and epoxy (with additive) systems have been selected for full scale flow measurements to determine the tube performance curves. To the extend the formulation and coating procedures had to be modified in order to achieve compatibility with application on the interior of PMMA tubes. The coatings could be applied on PMMA successfully and transparent systems have been obtained.

7.2 Coating analysis

The effect of hydrophobic coating can be significant as was demonstrated for the clean fluorinated coating. However, the window of material parameters for which the effect can be observed is narrow. A change in the flow patterns seems to occur for mildly hydrophobic surfaces, whereas a very high hydrophobicity seems to be required for reducing the pressure gradient at low gas flow rates as well (i.e. in the inverted churn flow regime). Hydrophobic materials are tested in the range of $\sim 55^\circ < CA_{\text{rec}} < \sim 140^\circ$, but only the Fluorinated coating ($CA_{\text{rec}} = \sim 105^\circ$) showed a good reboundability in the droplet impingement test as well as a significant reduction of the pressure gradient at low gas flow rates in the flow loop test.

There are indications that a (small) contamination layer deteriorates the positive effects (i.e. the reduction in the pressure gradient) of a hydrophobic coating easily. A contamination layer seems to be the result of using tap-water instead of ultra-pure water, and this formed rather quickly (order of hours). Although this process is reversible for the current situation, for applications in actual wells, where deposition is likely to be more severe, the effects of contamination puts extra limitations on coating applications. The contamination seem to result in pinning of the droplets to the wall upon impact, which counters the effect of hydrophobicity.

Comparing the results of the contaminated Fluorinated coating with the base case (i.e. PMMA) shows clearly that a change in the flow pattern is not directly coupled to a significant change in the pressure gradient.

The onset of liquid loading (i.e. the gas flow rate at which liquid appears below the liquid feed) is not significantly affected by a hydrophobic coating. This has been observed in previous projects as well.

The results of the droplet impingement tests seem to correspond well with the flow loop tests, and thus can be a simple and quick method for assessing the functionality of the coating.

Regarding the hypotheses posed in Chapter 3 :

I. Increasing the receding contact angle, increases the reboundability of droplets impinging on a surface.

A high CA_{rec} ($> \sim 100^\circ$) seems to be required to show a significant rebound during impingement tests. However, surface roughness seems to deteriorate this effect due to pinning of the droplets.

II. Increasing the reboundability of droplets from the pipe wall reduces the accumulation at the wall (i.e. reduces film formation), causing a change in flow patterns.

This is not completely true, since the contaminated Fluorinated coating shows poor reboundability, but still changes the flow patterns. Its receding contact angle is second best for all surfaces tested, hence a better statement seems to be: a receding contact angle above $\sim 70^\circ$ is required to obtain inverted-churn flow. This could be verified with additional tests.

III. Under conditions of droplet flow or inverted-churn flow, a more elastic rebound of droplets, reduces the momentum-loss to the wall, hence the pressure gradient.

A reduction of the reboundability in the impingement test for the contaminated Fluorinated coating compared with the clean Fluorinated coating coincides with an increase of the pressure-gradient. It is noted here that the presence of an inverted-churn flow does not necessarily result in a reduced pressure gradient compared to a 'normal' churn flow.

8 References

1. Belfroid, S.P.C, et al, *Effect of tube wall wettability on the onset of churning in upward gas-liquid annular flow*, OMAE2014-24687, 2014.
2. Chen, L. et al., A comparative study of droplet impact dynamics on a dual-scaled superhydrophobic surface and lotus leaf, *Applied Surface Sci.* 257, pp 8857-8863, 2011.
3. Khosla, V., Visual investigation of annular flow and the effect of wall wettability, MSc thesis TUDelft, 2012.
4. Khosla, V. et al, *Effect of wall wettability on gas-liquid upward annular flow*, ICMF 8, 2013.
5. Shell Liquid loading Game Changer projects
 - a Belfroid, S.P.C., Cargnelutti, M., *Modify Tubing Wall to Delay Film Reversal*, TNO report, Shell Liquid loading Game Changer I, 2009.
 - b Belfroid, S., Cargnelutti, M., Veltin, J., Schiferli, *Influencing liquid loading point*, Shell Liquid loading Game Changer II, 2010.
 - c Alberts, G., Belfroid, S., Groen, J., Turkenburg, D., *Delaying the onset of liquid loading by tubing wall modification through hydrophobic coating: pilot-scale experiments in the Donau Loop and laboratory tests of alternative coatings*, Shell Liquid loading Game Changer III, 2012.
 - d Nennie, E., Groen, J., *Delaying the onset of liquid loading by tubing wall modification through hydrophobic coating: laboratory-scale experiments for varying inclination angles*, TNO report, Shell Liquid loading Game Changer IV, 2013.
6. Takamasa, T., et al., *Experimental Study of gas-liquid two-phase flow affected by wall surface wettability*, *Int. J. Heat and Fluid Flow* 29, pp 1593–1602, 2008.
7. Veeken, C.A.M., Belfroid, S.P.C., *New Perspective on Gas-Well Liquid Loading and Unloading*, SPE 134483, 2010.
8. Westende, J.M.C. van 't, *Droplets in annular-dispersed pipe-flows*, PhD thesis TUDelft, 2008.

9 Signature

Delft, 19 februari 2016

TNO

G.J.N. Alberts
Manager HTFD

J.M.C van 't Westende
Author

D. Turkenburg
Author

A Droplet impingement tests

According to Chen et al. (ref. 2), who performed impingement tests with superhydrophobic surfaces ($CA = \sim 165^\circ$), droplets impacting on a surface will rebound if their impacting velocity exceeds a critical value given by :

$$V_c = \sqrt{\frac{\sigma |\cos \theta_{adv} - \cos \theta_{rec}|}{\rho R}}$$

Where ρ and R are the density and radius of the droplet, and σ is the surface tension of the liquid.

The reciprocal dependency of the critical impacting velocity with the droplet radius is rather counter-intuitive, since smaller droplets deform less easily and are wetting a smaller part of the surface upon impact, hence should rebound more elastically.

Using the equation given above, the critical impacting velocity reaches a maximum value for an advancing contact angle of $CA_{adv} = 90 + \frac{1}{2} (CA_{adv} - CA_{rec})$. In Figure A.1 this maximum value of the critical velocity is presented as a function of $(CA_{adv} - CA_{rec})$ for a droplet diameter of 5.2 mm.

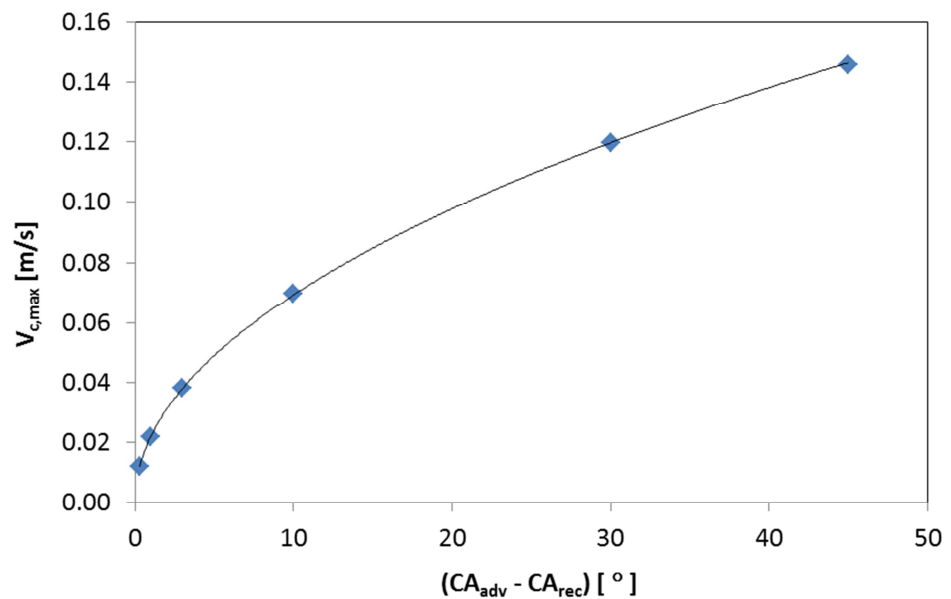


Figure A.1 Maximum value of the critical impacting velocity as a function of the difference between advancing and receding contact angle for a 500 μ m diameter water droplet. $V_{c,max}$ occurs at $\theta_{adv} = 90 + \frac{1}{2} \Delta\theta$.

For all surfaces studied, the impacting velocity has been well larger than their critical velocity, but a significant rebound does not occur, in general. The equation given by Chen et al. may not be suitable for mildly hydrophobic surfaces.